J Wood Sci (2014) 60:313–320
DOI 10.1007/s10086-014-1412-4

ORIGINAL ARTICLE

Changes in wood temperature under high-speed friction

Ryuichi Iida · Tadashi Ohtani · Takahisa Nakai · Koji Adachi

Received: 3 March 2014 / Accepted: 23 May 2014 / Published online: 5 July 2014

Abstract Thermal effects at the surface of a sample wood specimen while it is rubbed by reduction with a metal disk rotating at high speed are investigated. The results provide fundamental data for the development of new surface processing methods. The results of high-speed friction tests showed that the wood surface developed high-temperature regions due to the effect of friction heat, and deformed tissue was observed at the wood surface in the region that experienced the rubbing action. The thermal effects extended to a deep range in the deformed region by reduction due to different fiber inclination angles, both parallel and normal to the friction surface. The thermal effects from the rubbed conditions of the reduction and feed speed also extended deeply into the region deformed by reduction, although the thermal effect was decreased at higher feed speed. From the results of these friction tests, the change in wood temperature is described unambiguously by factors related to pressure on the friction surface.

R. Iida
Division of Human Life and Technology Education, The United Graduate School of Education, Tokyo Gakugei University, 4-1-1 Nukuikitamachi, Koganei-shi, Tokyo 184-8501, Japan

T. Ohtani (✉)
Department of Natural Science, Tokyo Gakugei University, 4-1-1 Nukuikitamachi, Koganei-shi, Tokyo 184-8501, Japan
e-mail: t-ohtani@u-gakugei.ac.jp

T. Nakai
Interdisciplinary graduate school of Science and Engineering, Shimane University, 1060 Nishikawatsu-cho, Matsue-shi, Shimane 690-8504, Japan

K. Adachi
Institute of Wood Technology, Akita prefectural University, 11-1 Kaieizaka, Nosiro-shi, Akita 016-0876, Japan

Keywords High-speed friction · Wood temperature · Thermal effect · Deformation effect

Introduction

Bent and compressed wood can be produced by processing methods involving heat application. These processing methods are often used for furniture and residential flooring, because the processing methods allow plastic deformation and increased surface hardness [1]. Such heat application methods require specialized equipment as a heat source.

Practical research related to problems of such equipment has shown that the hardness of wood surfaces can be increased without a thermal source using friction heat generated by compressed on a metal roller rotating at high speed [2]. Other practical research has reported on welding of wood samples by friction heat from microvibrations [3, 4]. This new processing method has been investigated for softening and welding wood surface tissue by means of friction heat.

On the other hand, in machining using a blade to cut wood, friction occurs between the workpiece and the cutting tool edge. The friction resulting from cutting the wood is a friction phenomenon resulting from contact between the wooden workpiece and the quickly moving blades of the tool.

McKenzie et al. [5] investigated friction phenomena like above cutting conditions between metal and wood. In that report, a wooden bar specimen was rubbed on the surface of a metal plate under a wide range of sliding speed conditions, and the friction coefficient was measured for various wood species and different surface pressures. The other research reported that the friction coefficient between

Swedish wood species, and steel was measured under different moisture content, sliding speed, and steel roughness [6].

Murase [7] also measured the friction coefficient between sliding wood and a heated metal plate, and the effect of temperature was discussed in changes of the friction coefficient. The other his report [8] was mentioned that the friction coefficient was measured by rubbing the wood specimen on a metal disk rotated at the wide range of 1–50 m/s under some assumptions about practical cutting conditions.

The above-mentioned research investigated friction coefficients under practical cutting conditions of high-speed friction between the tool and wood. However, these studies do not evaluate the temperature change of the wood sample generated by the friction heat.

Okumura et al. [9] also investigated temperature changes of tools in contact with wood by measuring the internal temperature of a metal bar specimen rubbed on a wood disk rotating at 14 m/s and using these measurements to estimate the temperature increase at the round bar tip. The temperature of the rubbed wood disk was not measured. Most previous research on cutting conditions between wood and tools have not focused on the temperature change in the wood during processing, instead examining friction coefficients between wood and tool, and temperature changes in the tool. There is thus a lack of fundamental research data regarding wood temperature changes from friction heat, despite practical uses of friction heat in wood processing and for friction properties of wood, such as friction coefficients.

This study aims at research and development of new wood processing methods that apply thermal effects to the surface layer of the wood by utilizing friction heat to produce new functionality at the wood surface. As a first step, the effects of friction heat are investigated at the surface layer of wood pressed against a metal disk. The detailed internal effects of wood temperature changes due to friction heat are also a focus of this study. Fundamental data are needed for developing new processing methods, and it is the aim of this study to provide them.

Materials and methods

Sample material

The material used in the experiments was air-dried Spruce with 10.3 % moisture content and 0.46 g/cm^3 density. The average annual ring width was 2.1 mm. Moisture content should be a considerable factor in this experiment due to the material characteristics of wooden self-lubrication with moisture. Therefore, this experiment was conducted in limited condition of the air-dried wood sample. The specimen (Fig. 1a, b) was 3 × 85 × 11 mm, cut from the sample material by a small circular saw, and the rubbed surface was set in the section of 3(width) × 85(length) mm.

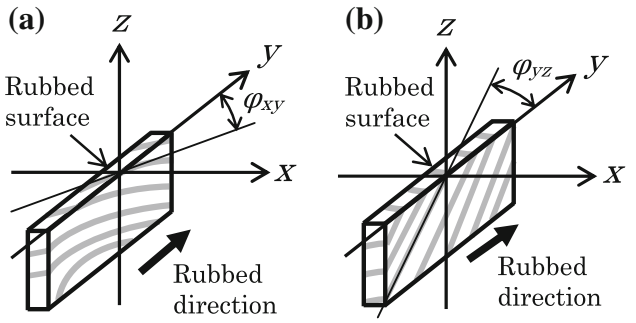

Fig. 1 Definition of rubbed surface for different inclination angles **a** φ_{xy} and **b** φ_{yz} with regard to grain of test specimens

The specimen was prepared with fiber inclination angles φ_{xy} and φ_{yz}, as shown in (a) and (b) of Fig. 1, respectively. φ_{xy} on the friction surface was set in 45°, 90°, or 135°, and φ_{yz} was 15°, 45°, 90°, 135°, or 165°. The 15° and 165° were added to φ_{yz} condition because compression strength was affected by small changes in fiber inclination angle of wood.

Experimental apparatus of friction test

Figure 2a, b shows a schematic illustration of the high-speed friction test apparatus and the detailed conditions of the rubbing system. As shown in Fig. 2a, the apparatus was configured to rub the rapidly rotating tool on the specimen surface while feeding the specimen by a uniaxial movable stage equipped with a dynamometer. The feed direction of the test specimen was used in the up-milling mainly of this experiment, because such rotating direction is being used widely in production line such as wood machining. Figure 2b shows the contact conditions of the tool and the test specimen. The reduction rate of the test specimen pressed against the tool surface is denoted by t. The rotation speed of the tool and the feed speed are denoted by R and f, respectively.

Experimental conditions

Table 1 shows the conditions of the friction test. The tool was made from carbon tool steel with a smooth surface (mean roughness: 1.8 μm). The diameter was 50 mm. The high-speed friction test used an upper method, feeding the sample specimen in the direction opposite the direction of tool rotation. The rotational speed of the tool was $R = 10\,000$ rpm. The specimen feed speed ranged from

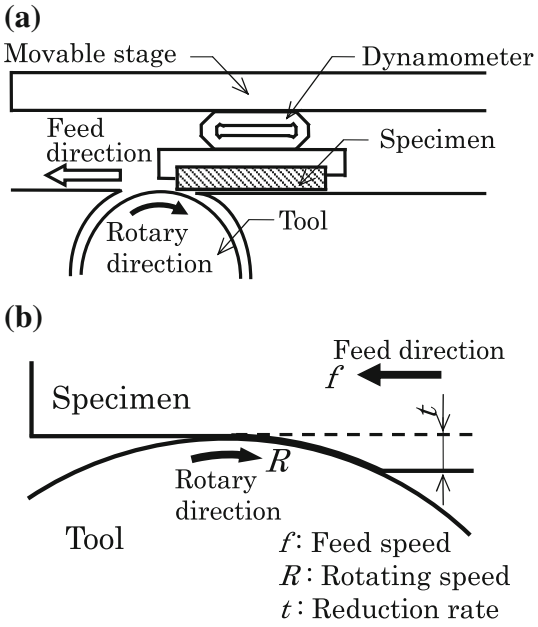

Fig. 2 Schematic illustration of **a** friction test apparatus and **b** details of the rubbing conditions

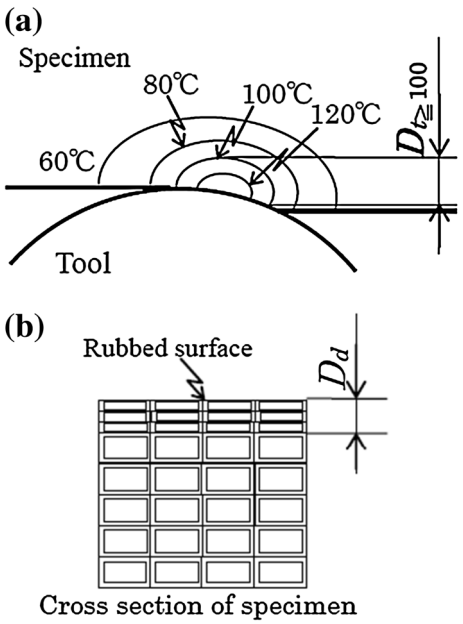

Fig. 3 Analysis method for depth of thermal effect (D_t) and depth of deformation (D_d)

Table 1 Friction test conditions

Tool and specimen	Condition (unit)
Tool material	Carbon tool steel
Tool diameter	50 (mm)
Tool surface roughness (R_a)	1.8 (μm)
Rotation speed of tool (R)	10000 (rpm)
Feed speed of specimen (f)	0.5, 2, 3, 4.5, 6 (mm/s)
Compression rate (t)	300, 500, 700 (μm)

$f = 0.5$–6 mm/s, and the reduction rate ranged from $t = 300$ to 700 μm.

The trial of high-speed friction test was conducted using the five pieces of spruce test specimen in each condition. After the friction test, the adhered brown stain was observed on the tool surface caused by extractives of the test specimen. Therefore, the tool surface was cleaned with ethanol just before each trial. In the friction test, the surface pressure P applied to the test specimen was calculated from the vertical and horizontal forces measured relative to the feed specimen.

Evaluation of thermal effect

To evaluate temperature change in the wood test specimens during the high-speed friction tests, the surface temperature of each test specimen was measured by a non-contact method from the side (relative to the feed direction of the specimen). The surface temperature was also evaluated by an infrared thermographic camera (TH6300R, Nippon Avionics Co., Ltd.), measured approximately 150 mm from the side surface of the specimen.

The emissivity of the wood specimen surface was set in 1. All experiments were performed out of the path of direct sunlight.

Analysis of thermal and deformation effects

After the high-speed friction test, a thermal image was obtained from the infrared thermography temperature image of the wood test specimen. Five thermal images were taken at intervals of 15 mm in a longitudinal direction, starting from the edge face of the specimen. The thermal image displayed a color-coded distribution at 10 °C intervals. To obtain detailed information of the temperature distribution in the thermal image, temperature change in the wood test specimens was evaluated using a temperature distribution map according to the isothermic temperature.

Figure 3a, b show the method for analyzing the thermal effects and depth of deformation region. Figure 3a shows the evaluation method for the thermal effect using the temperature distribution diagram. Previous researches were reported that the thermal softening behavior of water-saturated spruce sample occurs at range approximately from 80 to 100 °C [10] and of the lignin in air-dried condition occurs at approximately 100 °C [11]. From above review, this study focused on the region with temperatures

exceeding 100 °C. Thus, the high-temperature regions are defined as those with temperatures exceeding 100 °C, and the depth at which the high temperature of the temperature distribution diagram was seen is denoted D_t.

Figure 3b shows the method for evaluating the deformation effect in the depth direction. The deformation effect region was evaluated from the result of microstructure observations of the wood specimen after the friction test. The microstructure was observed using a scanning electron microscope (SEM) to observe cross sections (relative to feed direction) of the wood specimens. From the SEM images, the deformation range was taken to be the depth to which cell wall deformation can be observed, and the depth of the deformed region was denoted by D_d for the depth direction from the friction surface.

Results and discussion

Temperature distribution and deformed tissue of surface layer in wood sample

The high-speed friction test was conducted under the conditions of reduction rate $t = 300$ μm, feed speed $f = 0.5$ mm/s, and fiber inclination angles φ_{xy} and φ_{yz}. Figure 4 shows the rubbed surface of the wood sample specimen after friction test. Some of these rubbed surfaces change to be dark, and the color of the surface becomes darker as the φ_{yz} inclines versus the friction surface, especially the late wood of the surface darker.

Figure 5 shows the example of the actual color image obtained from the infrared thermography. The color image is displayed a color-coded temperature distribution at 10 °C intervals and used to make the temperature distribution map.

Figure 6 shows examples temperature distributions for wood sample specimen surfaces with fiber inclination angles $\varphi_{xy} = 0°$–$135°$ and $\varphi_{yz} = 0°$.

High-temperature regions exceeding 100 °C are observed at depths exceeding 500 μm from the contact surface under different fiber inclination angles φ_{xy}. The thermal effect region tends to spread in an elliptical shape regardless of the fiber directions. The value of the maximum temperature remains around $T_{max} = 125$ °C, and the maximum temperature does not vary significantly with changes in inclination angle φ_{xy}.

Figure 7 shows example temperature distributions for surface temperatures of the sample specimen at $\varphi_{xy} = 0°$ and $\varphi_{yz} = 0°$–$165°$. The sample test specimen is affected by the anisotropy of the different fiber inclination angles, and the thermal effect region tends to spread in concentric circles, appearing as elliptical shapes in the horizontal direction. The temperature of the near-contact surface is higher as the fiber direction inclines versus the friction surface, reaching $T_{max} = 160$ °C at $\varphi_{yz} = 90°$.

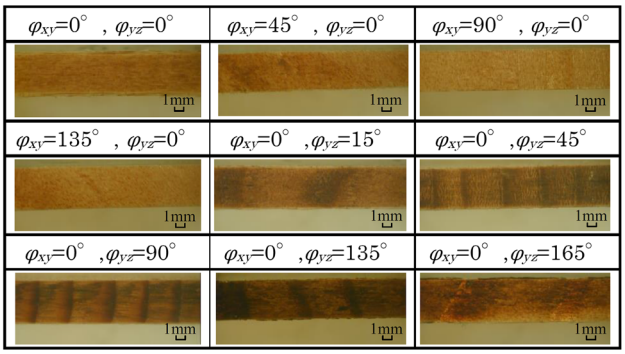

Fig. 4 Surface of wood sample specimen after friction test

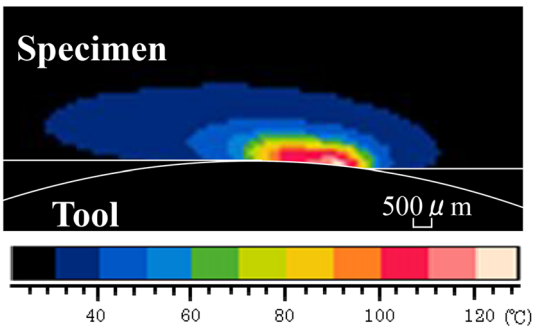

Fig. 5 An example of the thermal image at inclination angle $\varphi_{xy} = 0°$ and $\varphi_{yz} = 0°$

A high-temperature region appears at approximately 500 μm from the near-contact surface when the spruce sample specimens at the different inclination angles parallel and normal to the friction surface, such as φ_{xy} and φ_{yz} in Fig. 1 are rubbed by the metal disk under pressure, and the increase of internal temperature and the shape of temperature distribution of the specimen depend on the anisotropic effect of the fiber direction.

Figure 8a–f show example SEM images for various directions of cross-sectional reduction at different inclination angles parallel and normal to the friction surface. Figure 8c also shows the transverse section, in which deformation of the cellular tissue is observable because the deformation effect region is difficult to analyze in parallel fiber orientation to the vertical cross section.

As shown in Fig. 8a–c, cellular tissue is affected by reduction in the depth direction, and densified layers of cells can be observed to about 50 μm from the friction surface in the cross section. As shown in Fig. 8d–f, the depth of densification area increases with increasing the fiber inclination angle φ_{yz}.

The above results indicate that the vicinity of the contact surface reaches a high temperature when spruce sample specimens at different inclination angles parallel and normal to the friction surface are rubbed by the metal disk under pressure and that deformation also occurs at near-

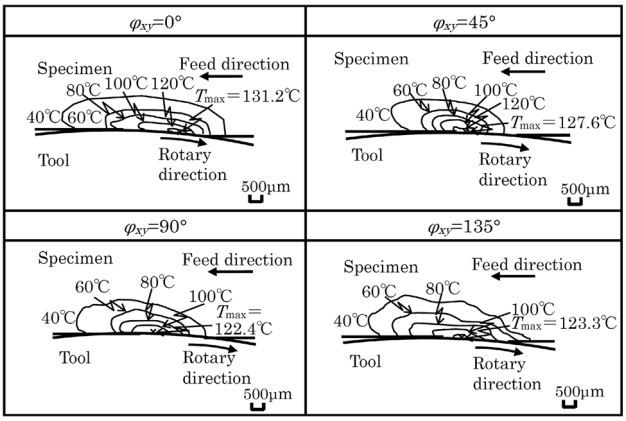

Fig. 6 Temperature distribution images at different inclination angles φ_{xy} of the sample test specimen

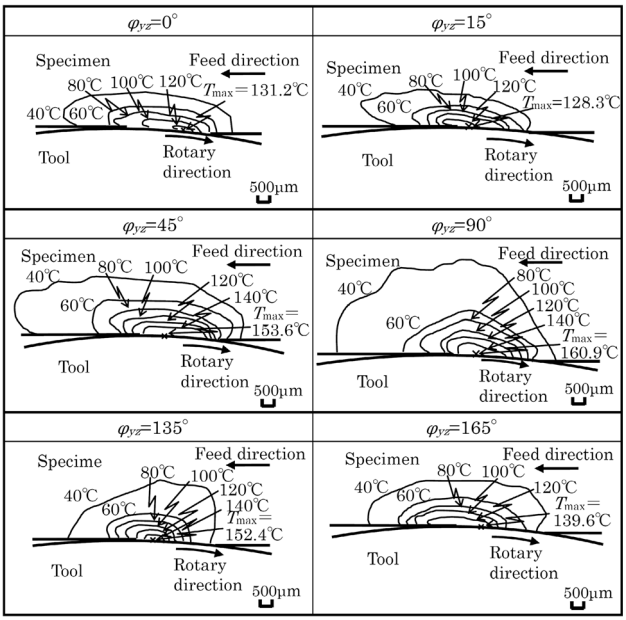

Fig. 7 Temperature distribution images for different inclination angles φ_{yz} of the sample test specimen

contact surfaces. The above results also indicate that anisotropy affects the thermal and densification effects.

Internal thermal effect of wood under high-speed friction

This section investigates details of the thermally affected area when a spruce sample specimen is rubbed with high-speed friction by a metal disk.

Figure 9 shows D_d and D_t in the cross-sectional structure and internal thermal effect regions according to analysis of data from the spruce test specimens at different inclination angles parallel to the friction surface. The values of D_d and D_t shown in Fig. 3a, b indicate the depth of deformation and thermal effects due to temperatures exceeding 100 °C, from analysis of data from the five sample test specimens.

The values of D_t and D_d shown in Fig. 9 are nearly constant for different inclination angles parallel to the friction surface. The ratio D_t/D_d is also constant at about 10 despite variations in angle φ_{xy}. This indicates that the thermal effects reach a sufficiently deep region relative to the depth of the deformed structure.

Figure 10 shows D_d and D_t in the cross-sectional structure and internal thermal effect regions at different inclination angles normal to the friction surface. At various inclination angles of φ_{yz}, D_d and D_t are largest at $\varphi_{\mathrm{yz}} = 90°$, and the effects of the thermal and deformed regions are deepest. The ratio D_t/D_d is also constant at about regardless of angle φ_{yz}, as with varied inclination angles parallel to the friction surface. These results indicate that the thermal effect reaches a sufficiently deep region relative to the depth of the deformed structure, even though the thermal effect varies with fiber inclination angle. The thermal and deformation effects also change in different fiber inclination angles, thus the effects might be varied by the wood surface tissue, such as the structure of early and rate woods.

The above results indicate that the internal thermal effect extends to a sufficiently deep range relative to the deformation effect by reduction when the spruce sample specimen is rubbed at various fiber inclination angles both parallel and normal to the friction surface.

Effect of rubbed condition on thermal distribution and deformed surface layer of wood

To investigate the detailed effects of friction, spruce sample specimens were subjected to high-speed rubbing with a metal disk under different feed speeds and reduction rates.

Figure 11 shows the relationship between feed speed f and internal maximum temperature $T_{\max}$ under various values for f and reduction rate t at fiber inclination angles of $\varphi_{\mathrm{xy}} = 0°$ and $\varphi_{\mathrm{yz}} = 0°$.

The value of $T_{\max}$ under reduction rate t is higher at lower f, and the value tends to decrease as f increases. The value of $T_{\max}$ is nearly constant at higher feed speeds, but increases at lower feed speeds as t increases. The value of D_t/D_d over the thermal effect range decreases to 5 from about 10 as the feed speed increases.

The above results regarding the effect of rubbed condition indicate that the maximize friction heat is seen at the lower feed speeds, up to 160 °C as the reduction rate increases. It was also found that the effect of friction heat extends to a sufficiently deep range in the deformed layer in the cross-sectional structure, due to reduction of the

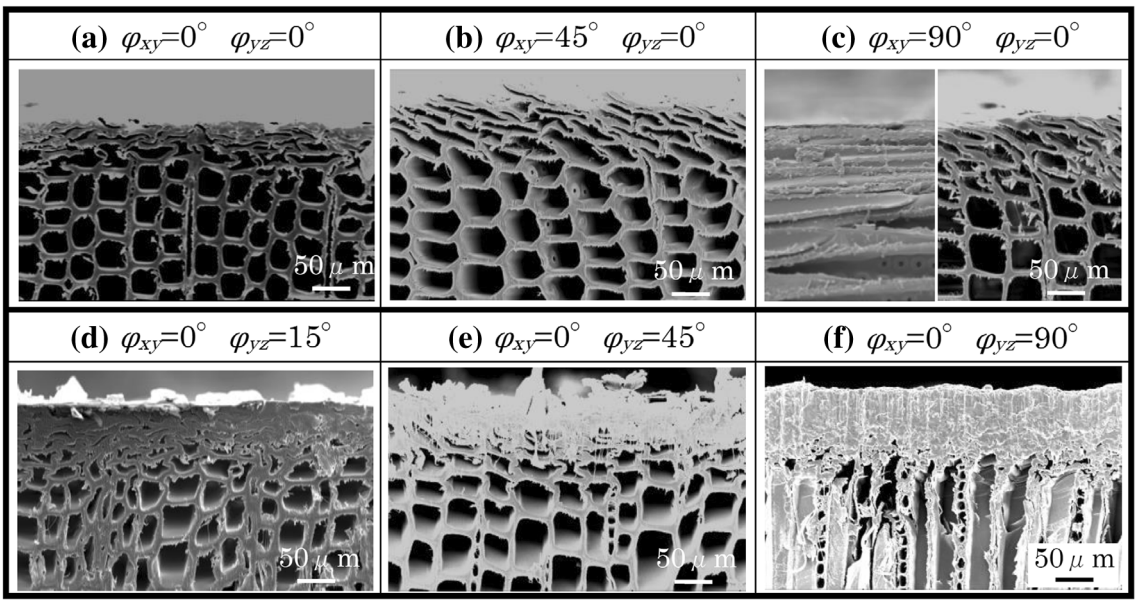

Fig. 8 SEM images of test specimens (*side view*) after the friction test **a–c** different inclination angles of φ_{xy} (**a**); **d–f** different inclination angles of φ_{yz}

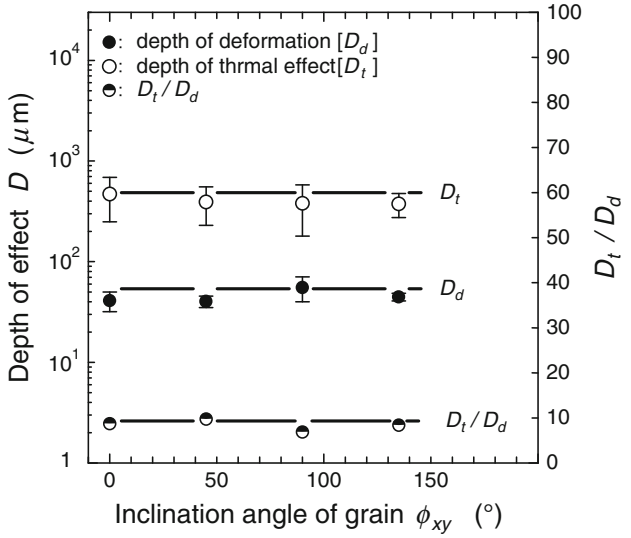

Fig. 9 Relationship between depth of deformation, thermal effect, D_t/D_d, and inclination angles of φ_{xy}

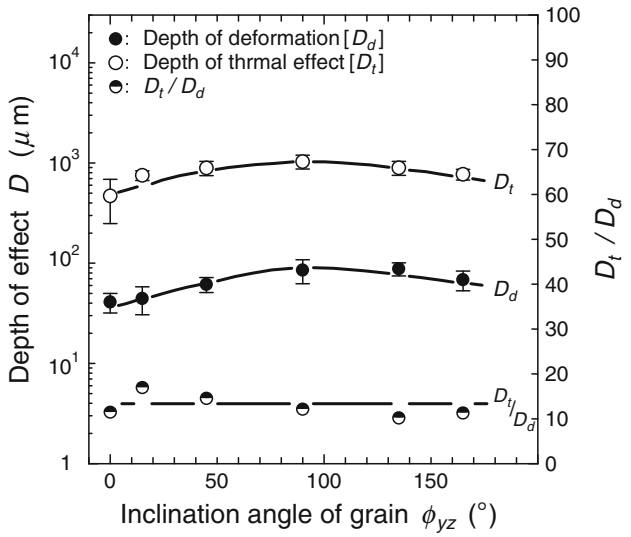

Fig. 10 Relationship between depth of deformation, thermal effect, D_t/D_d, and inclination angles of φ_{yz}

surface. Here, the results of feeding specimen in the down-milling direction were followed: the average value of $T_{\max}$ for the down-milling scattered in ranges of ±7 and ±4 % to that of the up-milling under both conditions of $f = 0.5$ mm/s and $f = 6$ mm/s, respectively. The average value of the variation coefficient in $T_{\max}$ was also 6 % in down-milling versus 3 % in that of up-milling under $f = 0.5$ mm/s. Also, the average value was 11 % in down-milling to 3 % in that of up-milling under $f = 6$ mm/s. From above result, it was considered that the $T_{\max}$ value between each feed direction was not so much difference in this experiment.

Effects of rubbed condition on wood temperature

Friction heat is affected by the feed speed and reduction rate when the wood sample is in contact with the metal disk tool which is high-speed rotating.

Such rubbed condition of friction test apparatus might be thought as similar in mechanism of metal rolling. The

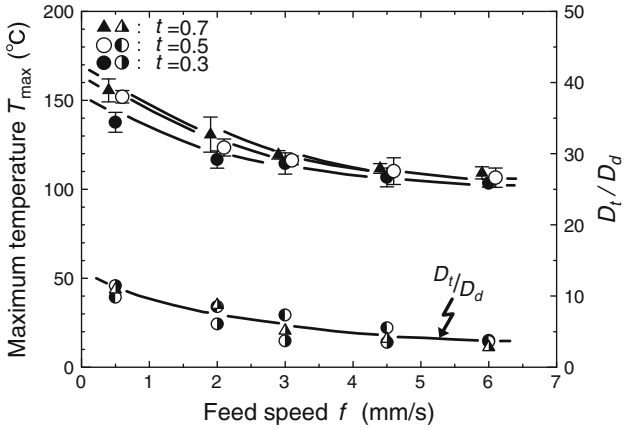

Fig. 11 Relationship between maximum temperature, D_t/D_d, and feed speed

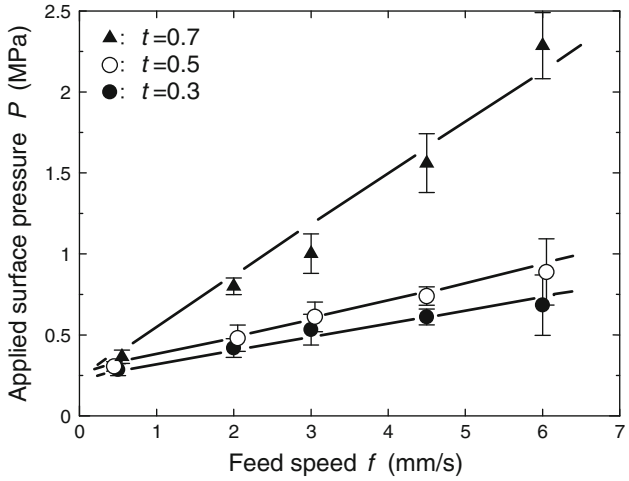

Fig. 12 Relationship between applied surface pressure and feed speed

forming technology of metal rolling can be controlled by the pressure applied to the product [12]. Therefore, the rubbed condition in this study can be thought as the factors to affect the applied pressure.

In focusing on the applied surface pressure by reduction and the relative speed between the wood and tool, this section investigates whether extracted factors related to friction affect the temperature change of wood.

Figure 12 shows the relationship between the applied surface pressure P, which is calculated from the horizontal and vertical component forces as measured by a dynamometer, and the feed speed f. The value of P applied to the friction surface increases linearly with f under each condition of the reduction rate t, and this tendency is remarkable at larger values of t. This indicates a possible explanation for why increasing the applied surface pressure raises the maximum temperature T_{max} by increasing the reduction rate. The relation between the feed speed and the speed of tool rotation is therefore examined, focusing on the applied surface pressure and how it is affected by changes in the reduction rate.

Previous research in wood machining reports that the operating parameter, such as the tool revolution speed, feed speed of workpiece, and numbers of teeth of tool are important for cutting wood [13].

Such relation of feed per tooth, in which the feed speed is divided by the numbers of teeth multiplied by the tool rotating speed, is often used for evaluation of the operating parameter. Above relation of operating parameter can be also related to the rubbed condition of feed per tool rotating speed. Therefore, the value of feed per rotating speed is calculated and the factors related to pressure on the friction surface is discussed.

Figure 13 shows the data of Fig. 12 rearranged according to the relationship between the maximum temperature T_{max} of the wood sample and the friction conditions

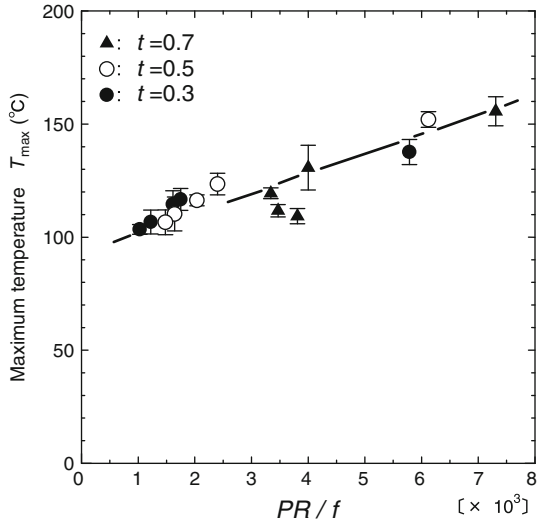

Fig. 13 Relationship between maximum temperature and friction parameters represented by *PR/f*

represented by the values of P, R, and f. The value PR/f represents the pressure under the condition of f/R, as represented by f/R on the feed speed of the wood sample per tool rotating speed.

The value of T_{max} increases nearly linearly as PR/f increases with different reduction rates. The results indicate that the increase in internal wood temperature due to friction heat is affected by pressure, acting on the feed speed of the wood sample per tool rotation. As Fig. 13 shows, the correlation coefficient in relationship between T_{max} and PR/f was 0.90.

These results indicate that the change in wood temperature is described unambiguously by pressure conditions in

the friction surface, meaning that factors such as reduction rate, feed speed, and tool rotation speed that effect the change of the wood temperature can be extracted as factors. Therefore, the temperature of the rubbed surface can be varied by the condition of applied surface pressure. Such condition of the surface applied pressure might be affected by the wood species, changing as the density and the early and rate wood structure in the friction surface. The effect of wood species will be probably investigated in future task. The results might continue that the extracted factors are utilized for controlling the wood temperature in future new processing method.

Conclusion

Changes in wood temperature were examined under various conditions of high-speed friction between a spruce sample specimen and a metal disk tool. The obtained results were as follows.

1. The region near the contact surface of the wood sample specimen reached a high temperature of 100° or more, and deformation of the cellular structure occurred near the contact surface. Results also indicated that anisotropy affected thermal and densification effects.
2. The internal thermal effect of the wood sample specimen extended to a sufficiently deep range relative to the deformation effect by reduction of the fiber inclination angles both parallel and normal to the friction surface.
3. The internal thermal effect under different friction condition decreased as the feed speed increased, but the effect extended to a sufficiently deep range relative to the deformation layer in the cross-sectional structure due to reduction of the surface.
4. From result (3), the change in wood temperature under high-speed friction is described unambiguously by factors related to pressure conditions in the friction surface.

It would be necessary to investigate the effect of moisture content focusing on the wooden self-lubricating property. Furthermore, the wood surface properties after the high-speed friction should be also investigated on the future report.

Acknowledgments This work was supported by JSPS KAKENHI Grant Number 24658154 and Adaptable and Seamless Technology Transfer Program through Target-driven R&D, JST

References

1. Inoue M, Norimoto M, Otshuka Y, Yamada T (1990) Surface compression of coniferous wood lumber I: a new technique to compress the surface layer. Mokuzai Gakkaishi 36:969–975
2. Morita T, Yoshioka M, Murase Y (2000) Frictional finishing of sugi lumber with high-speed rotating roller (in Japanese). Mokuzai Kogyo 55:597–600
3. Stamm B, Natterer J, Navi P (2005) Joining wood by friction welding. Holz Roh Werkst 63:313–320
4. Mansouri HR, Pizzi A, Leban J-M (2010) End-grain butt joints obtained by friction welding of high density eucalyptus wood. Wood Sci Technol 44:399–406
5. Mckenzie WM, Karpovich H (1968) The frictional behavior of wood. Wood Sci Technol 2:139–152
6. Guan N, Thunell B, Lyth K (1983) On the friction between steel and some common Swedish wood species. Holz Roh Werkst 41:55–60
7. Murase Y (1979) Effect of temperature on friction between wood and steel (in Japanese). Mokuzai Gakkaishi 25:264–271
8. Murase Y (1980) Frictional properties of wood at high sliding speed (in Japanese). Mokuzai Gakkaishi 26:61–65
9. Okumura S, Ishii T, Noguchi M (1993) Temperature of rubbing surface between steel rod and wood and wood Composites (in Japanese). Bulletin Kyoto Univ Forests 65:339–346
10. Salmen L (1984) Viscoelastic properties of in situ lignin under water-saturated conditions. J Mater Sci 19:3090–3096
11. Takamura N (1968) Studies on hot pressing and drying process in the production of fiberboard III: softening of fiber components in Hot Pressing of Fiber Mat. Mokuzai Gakkaishi 14:75–79
12. The Japan society for technology of Plasticity (1993) Advanced technology for strip rolling. CORONA PUBLIDHING CO., LTD. Tokyo, Japan, pp144–145
13. Csanady E, Magoss E (2011) Mechanics of Wood Machining, 2nd edn. Springer, Berlin p53